HHS Public Access

Author manuscript

Proc SPIE Int Soc Opt Eng. Author manuscript; available in PMC 2021 August 09.

Published in final edited form as:

Proc SPIE Int Soc Opt Eng. 2018 February ; 10578: . doi:10.1117/12.2295613.

Multi-atlas segmentation of the hydrocephalus brain using an adaptive ventricle atlas

Muhan Shao[a], **Aaron Carass**[a,b], **Xiang Li**[a], **Blake E. Dewey**[a], **Ari M. Blitz**[c], **Jerry L. Prince**[a,b], **Lotta M. Ellingsen**[a,d]

[a]Department of Electrical and Computer Engineering, The Johns Hopkins University, Baltimore, MD 21218 [b]Department of Computer Science, The Johns Hopkins University, Baltimore, MD 21218 [c]Department of Radiology and Radiological Science, The Johns Hopkins University, Baltimore, MD 21287 [d]Department of Electrical and Computer Engineering, University of Iceland, Reykjavik, Iceland

Abstract

Normal pressure hydrocephalus (NPH) is a brain disorder caused by disruption of the flow of cerebrospinal fluid (CSF). The dementia-like symptoms of NPH are often mistakenly attributed to Alzheimer's disease. However, if correctly diagnosed, NPH patients can potentially be treated and their symptoms reversed through surgery. Observing the dilated ventricles through magnetic resonance imaging (MRI) is one element in diagnosing NPH. Diagnostic accuracy therefore benefits from accurate, automatic parcellation of the ventricular system into its sub-compartments. We present an improvement to a whole brain segmentation approach designed for subjects with enlarged and deformed ventricles. Our method incorporates an adaptive ventricle atlas from an NPH-atlas-based segmentation as a prior and uses a more robust relaxation scheme for the multi-atlas label fusion approach that accurately labels the four sub-compartments of the ventricular system. We validated our method on NPH patients, demonstrating improvement over state-of-the-art segmentation techniques.

Keywords

MRI; enlarged brain ventricles; hydrocephalus; segmentation

1. INTRODUCTION

The ventricular system of the human brain comprises four interconnected cavities: the left and right lateral ventricles, and the third and fourth ventricles. Within each ventricle is a network of blood vessels, called choroid plexus, that produce cerebrospinal fluid (CSF). In a healthy brain, CSF flows from the lateral ventricles into the third ventricle via interventricular foramina, and from the third to the fourth ventricle via the cerebral

Further author information: (Send correspondence to M. Shao) M. Shao: muhan@jhu.edu.

aqueduct. From the fourth ventricle, CSF can pass into the central canal of the spinal cord or into the subarachnoid space.

Normal pressure hydrocephalus (NPH) is a type of brain disorder caused by disruption of CSF flow, leading to the expansion of the ventricles and distortion of the brain shape. Typical symptoms of NPH include urinary incontinence, gait unsteadiness, and dementia.[1] The symptoms often overlap with other neurodegenerative diseases, like Alzheimer's disease (AD), or traumatic vascular diseases of the cerebrum. However, unlike other forms of dementia, NPH is treatable and the symptoms can be reversed to some extent, through shunt surgery or endoscopic third ventriculostomy (ETV) on properly selected patients.[1–3] However, it remains a challenge to diagnose those patients who will respond well to treatment.

Brain imaging is one method to diagnose NPH. The chronically dilated ventricles can be observed through magnetic resonance imaging (MRI). Examples of T1-weighted (T1-w) Magnetically Prepared Rapidly Acquired Gradient Echo (MPRAGE) images of NPH patients are shown in Fig. 1(a). NPH patients often present with disproportionally dilated ventricular system[4] and hence, it would be beneficial to have an accurate parcellation of the ventricular system into its sub-compartments to quantify the relative size of the different compartments. The parcellation could better characterize the ventricular pathology for individual patients and help in the treatment plan. It could also enable researchers to subgroup NPH cases and develop more systematic studies of the disease.

Ventricle segmentation algorithms can be classified into two main categories. The first category of methods treats the ventricular system as a single unit.[9–11] Although, some of them can be used to robustly identify the ventricular system they cannot be used to quantify disproportionate dilation of the ventricular system in NPH. The second category sub-divides the ventricular system into multiple compartments. Multi-atlas label fusion methods have shown they can segment and label the ventricular system into its four cavities[5,6] (right and left lateral, 3rd, and 4th ventricles). However, these methods often fail in pathological cases since they rely on good registration results between the atlas and subject images and the enlarged ventricles in NPH patients can cause significant errors in the registration process. In this work, we present an automatic brain segmentation method, providing 138 brain labels in the cerebrum and cerebellum while performing accurate ventricular parcellation even with greatly enlarged ventricles in NPH patients.

The proposed method, referred to as Multi-Atlas Labeling using an Adaptive Ventricle Atlas (MA-LAVA), makes improvements to the RobUst DictiOnary-learning and Label Propagation Hybrid (RUDOLPH) method,[7,8] a whole brain segmentation method designed for subjects with enlarged ventricles. RUDOLPH integrates the Subject Specific Sparse Dictionary Learning (S3DL) method[12,13] and the Multi-Atlas Label Propagation with Expectation-Maximization (MALPEM) method.[5] We have made critical improvements to this method in two ways: 1) We incorporate an adaptive atlas from an NPH-atlas-based segmentation to provide a prior for the multi-atlas label fusion framework; and 2) We compute a weighted distance based on image intensities to correct the anatomical prior where the atlas registration is inaccurate due to large deformations. In Section 2, we

provide details on the new method, MA-LAVA, and on all required pre-processing steps. Section 3 includes our experiments on comparing our method with three state-of-the-art brain segmentation approaches, and Section 4 concludes the paper with a discussion of the presented work.

2. METHODS

2.1 Data preprocessing and atlases

The subject's T1-w MPRAGE image is N4 bias corrected,[14] rigidly registered to MNI 152 atlas space, and skull stripped using the method MONSTR.[15] The atlas cohort used in the initial multi-atlas registration consists of 15 T1-w MRI atlases with 138 manual labels from Neuromorphometrics Inc*. The NPH atlases used to create the adaptive NPH ventricle atlas were produced by manually delineating 5 T1-w MRIs of NPH subjects, each with 5 labels (the right and left lateral ventricles, third, and fourth ventricles, and a separate label representing all the remaining brain tissue). We classified the NPH patients into mild, moderate, and severe cases according to their ventricular volumes and chose NPH subjects for the atlas to range from mild to severe.

2.2 Multi-Atlas segmentation with an adaptive NPH prior

The first step of the proposed method is to register 15 Neuromorphometrics atlases into the subject's space, as is done in RUDOLPH. For this we use the SyN deformable registration method[16] and generate a probabilistic map $\Pi = \{\boldsymbol{\pi}_{ik}, i = 1,...,N, k = 1,...K\}$, where $\boldsymbol{\pi}_{ik}$ is the probability that a voxel i belongs to the label k. N and K represent the total number of voxels and labels, respectively.

The second step of the method is to create a subject specific adaptive ventricle atlas. This is done by processing the subject's MR image using the multi-atlas segmentation method MALPEM using 5 NPH images as atlases, each comprising 5 manual labels, as described in Section 2.1. The similarity between these 5 atlases and the subject provides a robust segmentation of the ventricular system for patients with enlarged ventricles. The output of this step is a hard segmentation $Z = \{z_i, i = 1,...,N\}$, where z_i is the label assigned for voxel i, including the left and right lateral ventricles, third ventricle, fourth ventricle, and the remaining brain tissue. This ventricle label map will be incorporated in the next step to correct any mis-registrations of the atlases and the subject image in the multi-atlas registration step.

To correct the anatomical prior from step 1, RUDOLPH adopts a relaxation framework from MALPEM and modifies it by accounting for the ventricular CSF label from S3DL.[5] This step in RUDOLPH is briefly described next (see details in Ref. 7). Assuming a Gaussian distribution, a parameter set (μ_k, σ_k) for each label k is estimated based on Π. The eight CSF-like labels within Neuromorphometrics are grouped together and build a common parameter set $(\mu_{\text{CSF}}, \sigma_{\text{CSF}})$. In RUDOLPH, Π is relaxed to Π^R as follows. At voxel i, where $\boldsymbol{\pi}_{ik}$ for at least one k is CSF-like, a fraction α_{ik} of the prior probability, $\boldsymbol{\pi}_{ik}$, is redistributed

* http://www.neuromorphometrics.com/

from label k to one of the eight CSF-like labels $k_{\mathrm{CSF},i}$, where $k_{\mathrm{CSF},i}$ is the CSF-like label with the highest prior probability or the CSF-like label of a voxel with the shortest Euclidean distance to i and that is marked as CSF in S3DL. In NPH patients with extremely large ventricles, both of these conditions sometimes fail in RUDOLPH when the prior from S3DL is inaccurate at the boundary of the enlarged ventricles. That is because at the boundary of the severely dilated ventricles the highest prior probability is often cortical CSF leading to the closest CSF-like label to become cortical CSF instead of the desired ventricular CSF.

In MA-LAVA we address this in two ways: 1) we look at the ventricular system segmentation Z from our adaptive NPH atlas; and 2) based on Z, we determine the CSF-like label by computing a weighted distance based on image intensities instead of the Euclidean distance. We identify the appropriate CSF-like label $k_{\mathrm{CSF},i}$ as

$$k_{\mathrm{CSF},i} = \begin{cases} z_i & \text{if } z_i \in \mathscr{C}_{\mathrm{MA}}, \\ \underset{k \in \mathscr{C}_{\mathrm{MA}}}{\operatorname{argmin}} \ \tilde{d}_k(i) & \text{otherwise}, \end{cases} \tag{1}$$

where $\mathscr{C}_{\mathrm{MA}}$ represents the CSF-like labels from the multi-atlas registration, and $\tilde{d}_k(i)$ is the weighted distance from the voxel i to the nearest voxel j with label k, which is defined as

$$\tilde{d}_k(i) = \sum_{n \in \text{line seg } ij} \lambda |I_i - I_n| \tag{2}$$

Here n is the voxel on the line segment that connects voxels i and j, I_i is the intensity of voxel i, and λ is a penalty factor. The weighted distance $\tilde{d}_k(i)$ is large if a ventricle CSF voxel goes through white matter voxels when searching for the closest CSF voxel. We follow the framework in RUDOLPH and MALPEM to calculate fraction α_{ik} based on the probability that the voxel with intensity I_i comes from either the intensity distribution $\mathcal{N}_k^{\prod}$ estimated by label k or $\mathcal{N}_{\mathrm{CSF}}^{\prod}$ estimated by label $k_{\mathrm{CSF},i}$,

$$\alpha_{ik} = \begin{cases} 0 & \text{if } \mathcal{N}_k^{\prod}(i) \geq \mathcal{N}_{\mathrm{CSF}}^{\prod}(i), \\ \max\left(0, \min\left(0.5 - \pi_{ik_{\mathrm{CSF,i}}}, \pi_{ik}\right)\right) & \text{otherwise}. \end{cases} \tag{3}$$

The relaxed prior Π^R is computed as

$$\pi_{ik}^R = \begin{cases} \pi_{ik} + \sum_{l \neq k_{\mathrm{CSF},i}} \alpha_{il} & \text{if } k = k_{\mathrm{CSF},i}, \\ \pi_{ik} - \alpha_{ik} & \text{otherwise}. \end{cases} \tag{4}$$

The relaxed prior Π^R is the initial input to an intensity-refined Expectation-Maximization (EM)[17] and is updated through an adaptive atlas framework.[10] The adaptive prior in iteration $t + 1$ is computed as

$$\pi_{ik}^{(t+1)} = (1-\kappa)\pi_{ik}^{R} + \kappa\left(G \star w_{ik}^{(t)}\right) \quad (5)$$

where G is a Gaussian kernel, κ is the adaption factor, π_{ik}^{R} is the original relaxed prior probability, and $w_{ik}^{(t)}$ is the posterior probability estimated in iteration t.

Smoothness is enforced with a global and stationary Markov Random Field.[18] The fusion-based (i.e., Π) and EM-based segmentations are eventually combined through a weighted scheme to estimate the final segmentation, as in RUDOLPH and MALPEM.

3. EXPERIMENTS AND RESULTS

To validate MA-LAVA, the parcellation of the ventricular system was done by following a manual delineation protocol[8] that uses the subject's T1-w MRI to identify the four sub-compartments of the ventricular system. In this work, a total of 41 subjects from mild to severe cases of NPH were delineated. We processed the 41 NPH subjects using MA-LAVA and three multi-atlas whole brain segmentation methods, MALPEM, Joint Label Fusion (JLF),[6] and RUDOLPH. Visual comparison (Fig. 1) of the three methods demonstrates that MA-LAVA provides a more robust segmentation, particularly on the boundary of the ventricles in NPH cases with extremely enlarged ventricles. We computed the Dice score[19] for the 41 NPH patients on the ventricular system segmentation. The results are reported in Table 1 and a visual comparison is shown in Figure 2. A paired Wilcoxon Signed-Rank Test[20] comparing JLF and MA-LAVA on the whole ventricular system has p-value <0.005. We get a p-value <0.0005 when comparing MALPEM and RUDOLPH to MA-LAVA on the whole ventricular system. MA-LAVA produces more accurate segmentation of the whole ventricular system and right and left lateral ventricles than MALPEM, JLF, and RUDOLPH. These results also show statistical significance (See detailed p-values in Table 2). We note that JLF gives better Dice scores of the third and fourth ventricles than MA-LAVA.

4. CONCLUSION AND DISCUSSION

We present refinements to a whole brain segmentation method that provides robust parcellation of the ventricular system in patients with enlarged ventricles. The new method, MA-LAVA, incorporates an adaptive NPH ventricle atlas as prior information for a multi-atlas label fusion framework and provides a new relaxation scheme to correct anatomical priors where registration-based segmentation fails due to large deformation. We validated our method on 41 NPH subjects and compared with three brain segmentation approaches. We have shown that MA-LAVA is more robust on identifying the boundary of the ventricular system across 41 NPH patients than MALPEM, JLF and RUDOLPH. We also demonstrated improvement in terms of overlap with manual delineations in lateral ventricles measured by Dice score. The significant improvements occur in severe cases of NPH patients, where the other algorithms fail to capture the boundary of the enlarged ventricular system.

Future work includes improvements when segmenting the third and fourth ventricles. This could be done by combining the lateral ventricle segmentations from MA-LAVA with the third and fourth ventricle segmentations from JLF. We also plan to subdivide the lateral

ventricles into subchambers (anterior, posterior, and inferior horns) to analyze the relative volumetric ratios within the ventricular system of NPH patients in greater details. The ultimate goal is to better understand the correlation between the volumetrics of these structures and the surgical outcomes for NPH patients.

ACKNOWLEDGMENTS

This work was supported by the NIH/NINDS under grant R21-NS096497, the National Multiple Sclerosis Society grant RG-1507-05243, the Department of Defense in the Center for Neuroscience and Regenerative Medicine, and the Icelandic Centre for Research (RANNIS) under grant 173942051.

REFERENCES

[1]. Williams MA and Relkin NR, “Diagnosis and management of idiopathic normal-pressure hydrocephalus,” Neurology: Clinical Practice 3(5), 375–385 (2013). [PubMed: 24175154]

[2]. Hakim S and Adams RD, “The special clinical problem of symptomatic hydrocephalus with normal cerebrospinal fluid pressure: Observations on cerebrospinal fluid hydrodynamics,” Journal of the neurological sciences 2(4), 307–327 (1965). [PubMed: 5889177]

[3]. Hopf NJ, Grunert P, Fries G, Resch KD, and Perneczky A, “Endoscopic third ventriculostomy: Outcome analysis of 100 consecutive procedures,” Neurosurgery 44(4), 795–804 (1999). [PubMed: 10201305]

[4]. Yamada S, Ishikawa M, and Yamamoto K, “Optimal diagnostic indices for idiopathic normal pressure hydrocephalus based on the 3D quantitative volumetric analysis for the cerebral ventricle and subarachnoid space,” American Journal of Neuroradiology 36(12), 2262–2269 (2015). [PubMed: 26359148]

[5]. Ledig C, Heckemann RA, Hammers A, Lopez JC, Newcombe VF, Makropoulos A, Lötjönen J, Menon DK, and Rueckert D, “Robust whole-brain segmentation: Application to traumatic brain injury,” Medical image analysis 21(1), 40–58 (2015). [PubMed: 25596765]

[6]. Landman B and Warfield S, “MICCAI 2012 workshop on multi-atlas labeling,” in [Medical Image Computing and Computer Assisted Intervention Conference], (2012).

[7]. Ellingsen LM, Roy S, Carass A, Blitz AM, Pham DL, and Prince JL, “Segmentation and labeling of the ventricular system in normal pressure hydrocephalus using patch-based tissue classification and multi-atlas labeling,” in [Proceedings of SPIE–the International Society for Optical Engineering], 9784, NIH Public Access (2016).

[8]. Carass A, Shao M, Li X, Dewey BE, Blitz AM, Roy S, Pham DL, Prince JL, and Ellingsen LM, “Whole Brain Parcellation with Pathology: Validation on Ventriculomegaly Patients,” in [International Workshop on Patch-Based Techniques in Medical Imaging], 20–28, Springer (2017).

[9]. Bazin P-L and Pham DL, “Topology-preserving tissue classification of magnetic resonance brain images,” IEEE transactions on medical imaging 26(4), 487–496 (2007). [PubMed: 17427736]

[10]. Shiee N, Bazin P-L, Cuzzocreo JL, Blitz A, and Pham DL, “Segmentation of brain images using adaptive atlases with application to ventriculomegaly,” in [Biennial International Conference on Information Processing in Medical Imaging], 1–12, Springer (2011).

[11]. Patenaude B, Smith SM, Kennedy DN, and Jenkinson M, “A Bayesian model of shape and appearance for subcortical brain segmentation,” Neuroimage 56(3), 907–922 (2011). [PubMed: 21352927]

[12]. Roy S, Carass A, Prince JL, and Pham DL, “Subject specific sparse dictionary learning for atlas based brain MRI segmentation,” in [International Workshop on Machine Learning in Medical Imaging], 248–255, Springer (2014).

[13]. Roy S, He Q, Sweeney E, Carass A, Reich DS, Prince JL, and Pham DL, “Subject-specific sparse dictionary learning for atlas-based brain MRI segmentation,” IEEE journal of biomedical and health informatics 19(5), 1598–1609 (2015). [PubMed: 26340685]

[14]. Tustison NJ, Avants BB, Cook PA, Zheng Y, Egan A, Yushkevich PA, and Gee JC, "N4ITK: Improved N3 bias correction," IEEE transactions on medical imaging 29(6), 1310–1320 (2010). [PubMed: 20378467]

[15]. Roy S, Butman JA, Pham DL, Initiative ADN, and others, "Robust skull stripping using multiple MR image contrasts insensitive to pathology," NeuroImage 146, 132–147 (2017). [PubMed: 27864083]

[16]. Avants BB, Epstein CL, Grossman M, and Gee JC, "Symmetric diffeomorphic image registration with cross-correlation: Evaluating automated labeling of elderly and neurodegenerative brain," Medical image analysis 12(1), 26–41 (2008). [PubMed: 17659998]

[17]. Van Leemput K, Maes F, Vandermeulen D, and Suetens P, "Automated model-based tissue classification of MR images of the brain," IEEE transactions on medical imaging 18(10), 897–908 (1999). [PubMed: 10628949]

[18]. Zhang J, "The mean field theory in EM procedures for Markov random fields," IEEE Transactions on signal processing 40(10), 2570–2583 (1992).

[19]. Dice LR, "Measures of the amount of ecologic association between species," Ecology 26(3), 297–302 (1945).

[20]. Wilcoxon F, "Individual comparisons by ranking methods," Biometrics bulletin 1(6), 80–83 (1945).

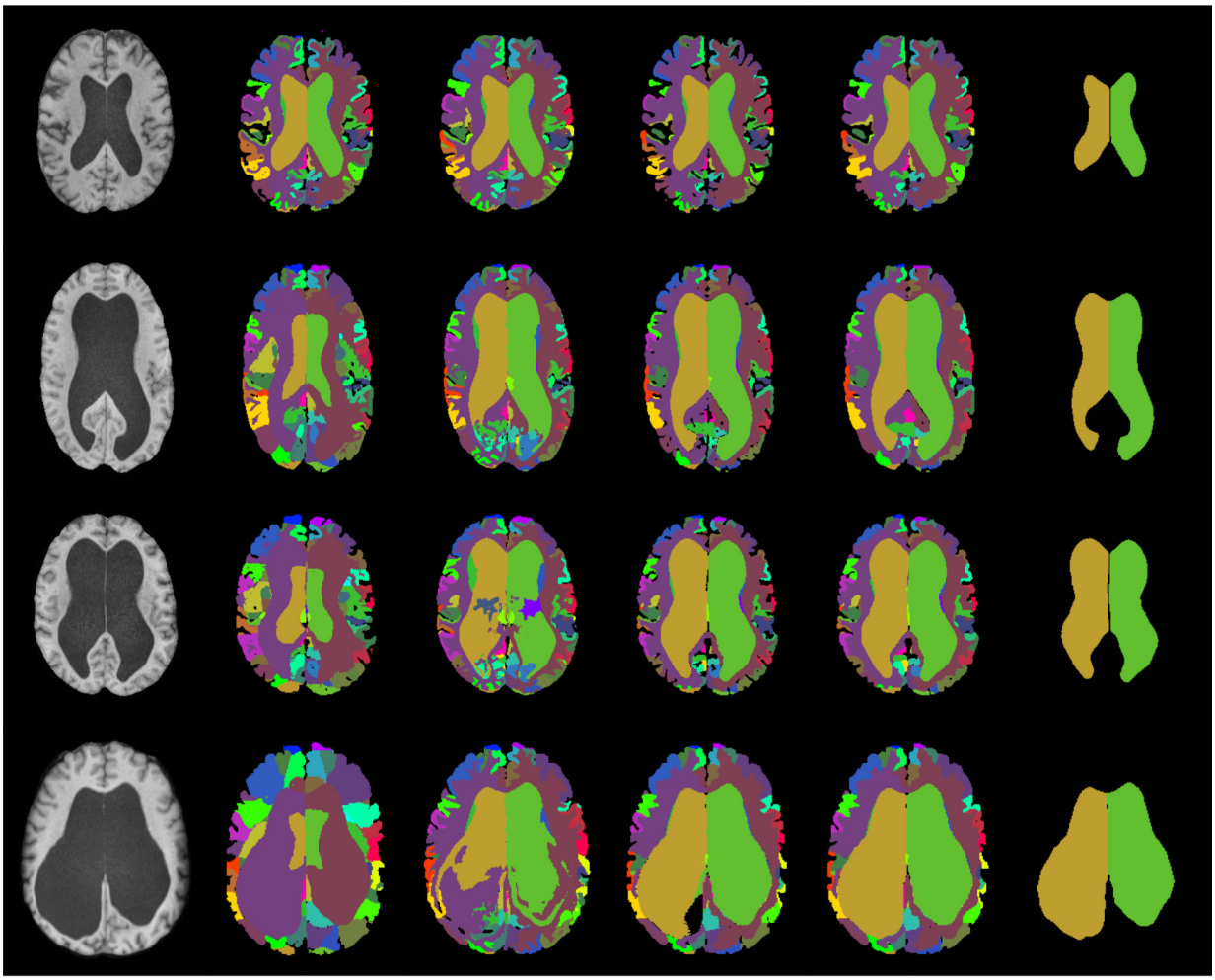

Figure 1.

(a) T1-w MPRAGE image of NPH patients. (b)-(f) show the ventricle segmentation generated by (b) MALPEM,[5] (c) Joint Label Fusion (JLF),[6] (d) RUDOLPH,[7,8] (e) MA-LAVA, and (f) Manual delineation (yellow/green is the right/left lateral ventricle).

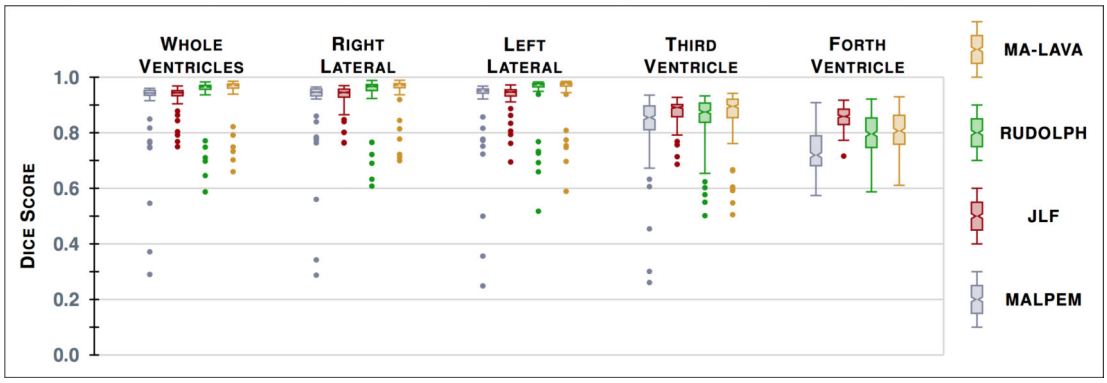

Figure 2.

Box plots of the Dice score[19] with our manual delineations over 41 NPH patients for the segmentation by the four methods, evaluated on the whole ventricular system and its four cavities.

Table 1.

The mean Dice score (and standard deviation) over 41 NPH patients measuring similarity between manual labels and automatically generated labels from the four methods. We compare four cavities of the ventricular system: right lateral ventricle (RLV), left lateral ventricle (LLV), third ventricle (3rd), and fourth ventricle (4th).

	MALPEM	JLF	RUDOLPH	MA-LAVA
Whole	0.8797(±0.1512)	0.9198(±0.0539)	0.9240(±0.1002)	0.9343(±0.0837)
RLV	0.8835(±0.1523)	0.9199(±0.0543)	0.9232(±0.0988)	0.9363(±0.0777)
LLV	0.8823(±0.1614)	0.9213(±0.0601)	0.9275(±0.1078)	0.9363(±0.0920)
3rd	0.7970(±0.1541)	0.8651(±0.0560)	0.8242(±0.1150)	0.8340(±0.1200)
4th	0.7227(±0.0846)	0.8503(±0.0438)	0.7904(±0.0769)	0.8079(±0.0753)

Table 2.

p-values for a paired two-sided Wilcoxon Signed-Rank Test[20] between the listed methods for the whole ventricular system and its four ventricle cavities across the 41 patients.

Comparison	Whole	RLV	LLV	3rd	4th
MALPEM vs. MA-LAVA	0.0003	0.0003	0.0013	0.2258	1.728e-11
JLF vs. MA-LAVA	0.0036	0.0015	0.0056	0.0616	0.0002
RUDOLPH vs. MA-LAVA	5.002e-11	9.056e-9	5.83e-8	0.0039	9.397e-7